THE EXPANSION CENTER MODEL
as a
CHALLENGE TO COSMOLOGY
-
based on data, results, and 3 historical models

by Luciano Lorenzi
XLVII Congresso Nazionale della SAIt
Trieste, 14-17 Aprile 2003

ABSTRACT

Challenge to cosmology is a paper which wishes to draw the astronomical community's attention to the manifest observational evidence for an expanding Universe from the center of the huge void of Bahcall & Soneira (1982), within the so-called "expansion center model" (ECM hereafter). Basic results from the application of the ECM equation are re-presented, together with independent well-established data as proof of the expansion direction. A further development of the ECM is proposed. After obtaining a quick derivation of $\dot{r}_{obs} = cz$, an algorithm based on fictitious luminous distances has been applied to a dipole test for 7 remote range-samples of Abell clusters of Richness 3. The confirmed dipole, according to the solution of the nearby Universe, gives absolute magnitudes which increase with square distance for the tenth brightest cluster member. Referring to the supernovae SNe Ia of the SCP (Perlmutter et al. 1999), one also finds the ECM agreement with the SCP result, and, as a further consequence, an empirical formula for the cosmological luminous distance D_C.

Finally a few physical considerations are advanced in a brief review of 3 important historical models.

1. Introduction

Sorry for the title! Indeed there must be some strong reasons for presenting a paper in such an aggressive manner; the first is tied to the hope of pressing the astronomical community to pronounce itself once and for all on clear experimental evidence for an expanding Universe from an expansion center, independently of theoretical and philosophical prejudices. A further reason is time. In fact 15 years have passed since the preliminary formulation of the expansion center model. It seems incredible that modern science has been so far untouched by a new reading of affirmed data able to support a different Universe from that imagined by theoreticians. It is likely that astronomical science is not yet as mature as physical science; otherwise we should think that the scientists' silence may be governed by other than scientific interests. Let me cite a clear proof of this. The revolutionary astronomical evidence for a new cosmology trend is not 15, but 30 years old, in that it has been accumulating ever since the historic, underestimated and misunderstood Rubin Ford Rubin effect, dated 1973! Thereafter an entire generation of theoreticians has dedicated itself to the defence of what has been authoritatively printed and based on 'sound' academic principles. However Nature and physics are not rational. They become so only after discovery, that is after the conquest and rationalization of what till that moment had been unknown. In other words, what is affirmed here is the simple supremacy of empirical science over theory alone. It has been the 20^{th}century's biggest mistake to believe the contrary. Theory can come only after observation. The reverse brings to mind the anthropocentric world of magic and religion; the mathematical approach to an idealized nature in platonic terms has to be condemned in the same way as other recent fundamentalisms. Such an introductive speech, which may sound too much like a lament to be generally shared, is not adressed to young scientists or promoters of space science; it would try to remind the temple guardians of official science of the inflexible verdict of scientific method, that must always be governed by experimental or observational verification. What cannot be verified has no right to citizenship in modern science. So the current challenge to cosmology has to be considered only as a kind invitation to astronomers to analyse and, if it is the case, to confute the observational evidence for the expanding Universe from a center, which here has been re-proposed within the so-called "expansion center model" (ECM hereafter).

2. The Controversial Cosmological Principle

As is well known to all, modern cosmology continues to base itself on the authoritative Cosmological Principle, which essentially excludes any possible center of the expanding Universe. Such a statement has till now received support through observation of cosmic homogeneity and isotropy on large scale. At the same time, the evidence of the

last few decades for anisotropies and deviation of the Hubble flow has been systematically interpreted as local effects doomed to disappear on a larger scale. Letting aside the historical reasons for adopting such a Cosmological Principle, after a few centuries of controversy about Man's position in the Universe, starting from Giordano Bruno's heretical philosophy and concluding with the recently discussed Anthropic Principle, we must here consider and analyse scientifically, on the grounds of available faithful observational data, the experimental consistency of "the idea that all observers, everywhere in space, perceive the Universe in roughly the same way regardless of their actual position (Chaisson, 1990)". Of course the previous statement represents an isotropical view of the Universe seen from any place, our Galaxy included. So, if we should find some particular direction, with respect to which a systematic phenomenon is observed at different distance ranges, the Cosmological Principle would be confuted by these observations. In practice this would mean that any other place might have another particular direction of observation, and that, if all these lines had the same origin point, only the observers located there would perceive the Universe to be roughly the same in any direction. Then such a point should be a special point ! The task of this paper is to remind the scientific community of the strong physical proofs about the real presence of this point that, as shown by the expansion center model (ECM), roughly coincides with the center of the huge void of Bahcall & Soneira (1982).

3. Data In Proof Of The Expansion Direction

The data which shows experimentally the real presence of a particular direction of expansion of our nearby (non-relativistic) Universe comes directly from observational cosmology; a list of some independent data is the following:

3.1 The historic RFR effect (1973)

In the mid-seventies a historic astronomical observation raised many perplexities regarding the full validity of the Hubble law (Nottale, Pecker, Vigier, Yourgrau, 1976). It was the so-called RFR effect (Rubin, Ford, Rubin, 1973), that showed an anisotropy of dipole type of the Hubble constant, through smaller observed Hubble ratios inside Region 1, with a concentration maximum approximately at $\alpha \sim 8^h/9^h, \delta \sim +20^\circ/+40^\circ$.

3.2 The Wedge-Shaped Hubble Diagram (1975)

In 1975 Sandage & Tammann (S&T hereafter) published their Paper V in which an accurate data listing of nearby galaxies was tabled and reported in a famous wedge-

shaped Hubble diagram, where the Hubble ratios appeared scattered between ~ 30 and $\sim 150\ Km\ s^{-1}Mpc^{-1}$. Another wedge-shaped velocity-distance diagram, with different symbols for different methods and a covered distance depth of about 200 Mpc, is the Rowan-Robinson one (1988); here the Hubble constant appears to lie in the range $50-80\ Km\ s^{-1}Mpc^{-1}$, with a current best value in the middle of this range. Of course the wedge-shape of the Hubble diagramm can be reasonably considered as due to an anisotropy of dipole type of the Hubble constant, to be verified in terms of the RFR effect.

3.3 A Huge Void centered at $\alpha_{VC} \approx 9^h, \delta_{VC} \approx +30^\circ$ (1982)

After the discovery by Kirshner (1981) of a large void in Bootes, Bahcall & Soneira (1982) carried out an accurate cosmographic analysis in which they described a $\sim$ 300 Mpc void of nearby catalogued rich Abell clusters of galaxies, extending 100° across the sky in the redshift range of $z \approx 0.03 - 0.08$, and centered approximately at $\alpha_{VC} \approx 9^h, \delta_{VC} \approx +30^\circ$ ($l_{VC} \approx 195^\circ, b_{VC} \approx +40^\circ$). As the void appears to extend $300h^{-1}Mpc$ by $\geq 60h^{-1}Mpc$, in projection, and to be $150h^{-1}Mpc$ deep (Bahcall, 1988), the distance of our Galaxy from the center of this huge cosmic structure (ovoid in appearance) results from $R_{MW} \approx (60 + 150/2)h^{-1}Mpc$, that, with an observed $h^{-1} \simeq 1.7 \pm 0.4$ toward VC (based on 1975 data by S&T), gives

$$R_{MW} \approx 135h^{-1}Mpc \simeq 230 \pm 54\ Mpc \tag{1}$$

3.4 Optical Dipole Anisotropy towards the void center VC (1987)

Very near to the void center VC one finds the direction of an optical dipole (Lahav 1987) (LOD hereafter) which points towards $l = 227^\circ \pm 23$, $b = +42^\circ \pm 8$. Such a dipole anisotropy in the galaxy optical distribution is based on about 15,000 galaxies, at the low average depth of $50h^{-1}Mpc$; it suggests, together with the IRAS result ($l = 248^\circ, b = 40^\circ$ by Yahil et al. 1986; $l = 235^\circ, b = 45^\circ$ by Meiksin & Davies 1986), that light traces mass.

3.5 A Great Wall towards the Huge Void (1989)

Evidence for large matter features surrounding the 'Huge Void', in the declination range $8^\circ < \delta < 44.5^\circ$ and $z \approx 0.02 - 0.03$, comes from the detection by Geller &

Huchra (1989) of many galaxies lying in thin sheet-like structures. The largest is the "Great Wall", with a minimum extent of $60h^{-1}Mpc \times 170h^{-1}Mpc$.

3.6 Persistence of Hubble Ratio Dipoles towards VC (1989-1999)

In conclusion of the paper (Lorenzi, 1999b) dealing with a "local solution of a spherical homogeneous and isotropic Universe radially decelerated towards the expansion center" an optional section entitled "Mini check atlas of Hubble ratio dipoles" was attached. These 7 plotted diagrams derived from 5 different samples of historic data sets, 1 by de Vaucouleurs (1965), 2 by Sandage & Tammann (1975), and 2 by Aaronson et al. (1982-86), as a whole referred to a distance range running from about 10 to 100 Mpc. In this wide range it is possible to observe an indisputable persistence of similiar Hubble ratio dipoles, by plots of Hubble ratios against $-\cos\gamma$, pointing towards the void center VC, for which $\gamma = 0$. Such a result is more spectacular than rigorous, according to the ECM; however it shows the regularity of the RFR effect at different distance ranges. Indeed many other Hubble ratio dipoles were obtained within the preliminary empirical model (Lorenzi, 1989, 1991); however, after the discovery (see Appendix in Lorenzi, 1994) of a high rate of variation of the Hubble constant in the nearby Universe a more rigorous mathematical formulation of the expansion equation was developed, which seemed to make the model extension to more distant and less accurate samples problematic. One of these is the homogeneous Abell sample of 66 clusters of Richness 3, at an approximate average distance of $\sim 500h^{-1}Mpc$ (Abell, Corwin, Olowin, 1988), that has been here (data are listed in **Table A** of the Appendix) employed as a key sample for testing a dipole formula based on fictitious luminous distances (see subsection 5.5).

4. Basic Results From The Expansion Center Model

After the above briefing of well-established data by observational cosmology it is time to show the most meaningful mathematical and numerical results obtained by the development and application of the ECM. As the majority of the results listed below derive from previous works (Lorenzi, 1999a,b hereafter referred as paper I and paper II), such results and their better understanding presume the knowledge of the contents of these references.

4.1 The new Hubble Law

After obtaining the general Hubble law

$$\dot{R} = HR \tag{2}$$

centred in the expansion center VC, from the trigonometrical formula of the observed distance r between our Galaxy MW and another galaxy or group/cluster/supercluster, one finds analitically the new observational Hubble law in the form

$$\dot{r} = Hr + \Delta H \cdot (r - R\cos\gamma) + R\dot{w}\sin\gamma \tag{3}$$

The eq. (3) can also be obtained very quickly by a vectorial approach, after putting $\alpha = 180° - w - \gamma$ with $\dot{w} = 0$ assumed, and writing $\dot{r}$ as

$$\dot{r} = (H+\Delta H)(R+\Delta R)\cos\alpha - HR(-\cos\gamma) \quad being \quad (R+\Delta R)\cos\alpha = r - R\cos\gamma \tag{4}$$

4.2 Physical interpretation given to ΔH

According to the ECM, and in agreement with the much acclaimed homogeneity and isotropy of the Universe, the finite difference $\Delta H = H_{ga} - H_{MW}$ taken as space effect at the epoch t_e is $= 0$. This means having the same Hubble constant everywhere contemporarily. The quantities H, r, R, γ are all snapshot quantities dating from the emission epoch t_e, hence belonging to the past snapshot that we observe only today; so such quantities do not vary during the light travel. Differently both ΔH and $\dot{w}$ refer to finite differences between points separated by light space, that is between the values at the emission point and those at the observation point. Then, after putting in first approximation $H \cong H_0 + K_0 r$, such a ΔH results to be

$$\Delta H \cong K_0 r \tag{5}$$

The formula (5) gives a physical interpretation to the observed Hubble ratio dipole, which originates from $K = \delta H/\delta r$, that is from the rate of variation of H to r. Consequently the ΔH value stems from a time effect, or light space effect, due to the delay of the light reaching the observer.

4.3 Search for partial interpretation of $R\dot{w}\sin\gamma$

The time effect above explained for ΔH can be found in the same way for $\dot{w}$. By analogy we can try to write, as a special case, $\dot{w} \equiv \dot{\theta}\cos\tau - \dot{\theta}_0\cos\tau$, only to represent intuitively the significance of $\dot{w}$ as the difference of a hypothetical common angular velocity between the observed galaxy at t_e and our Milky Way at t_0. So it would result

$$R\dot{w} \equiv R\Delta\dot{\theta}\cos\tau \tag{6}$$

, where $\Delta\dot{\theta}$ represents the expected variation of the Milky Way angular velocity, arising in the time elapsed during the light travel, and τ the inclination of the velocity vector $R\Delta\dot{\theta}$ to the direction $R\dot{w}$. Note that both $R\dot{w}$ and $R\Delta\dot{\theta}$ are velocity vectors perpendicular to the radius vector R, by definition, and their contribution to $\dot{r}$ in (3) vanishes toward $\gamma = 0°$ or $180°$ thanks to the factor $\sin\gamma$. A calculus attempt of the $\Delta\dot{\theta}$ expression has been carried out separately in a brief parallel paper (Lorenzi 2003a). Essentially eq. (6) represents the observable differential rotation of the Universe as a consequence of the light delay. However such an interpretation requires another necessary hypothesis, that is a rigid rotation of the Universe, with the absence of any differential rotation in space. In other words both the removal of the space effect for ΔH and $\Delta\dot{\theta}$ are necessary conditions of the ECM, according to a reshuffled or revised Cosmological Principle.

Indeed the previous is a very tangled problem to solve, like that of the peculiar velocities. Here only a partial and preliminary interpretation of $R\dot{w}\sin\gamma$ has been outlined. Therefore such a $\dot{w}$ contribution, as in paper II, will still be unconsidered in the following ECM application.

4.4 The ECM equation

The new Hubble law (3), with $\dot{w} \equiv 0$ assumed, after a few substitutions according to the formulas developed within the ECM, finds the most useful formulation, that following:

$$\frac{\dot{r}_{obs}}{r} = H_0 \left(\frac{1+x}{1-x}\right) - a_0 \cdot (1-x)^{-\frac{2}{3}} \cos\gamma \qquad (7)$$

where

$\dot{r}_{obs}$	observed radial velocity
r	space distance at the emission time
H_0	Hubble constant
$a_0 = K_0 R_0$	Galaxy radial deceleration coefficient ($= 3H_0^2 R_0/c = -3H_0 q_0$)
$-q_0 = H_0 R_0/c$	Galaxy recession velocity as dimensionless parameter
$x = 3H_0 r/c$	variable quantity whose value in the nearby Universe is $\ll 1$
$\cos\gamma$	variable quantity according to the observed position

4.5 The Hubble ratio dipole of the very nearby Universe

In the very nearby Universe eq. (7) becomes extremely simple. In fact, for $x \to 0$ then $r \to 0$, the expansion dipole results as

$$\frac{\dot{r}_{obs}}{r} \cong H_0 - a_0 \cos\gamma \tag{8}$$

or as the equivalent form

$$\frac{\dot{r}_{obs}}{r} \cong H_0(1 + 3q_0 \cos\gamma) \tag{9}$$

4.6 Explanation of the Wedge-Shaped Hubble Diagram

Always in the very nearby Universe the eqs. (8)(9) are able to explain the observed wedge-shaped Hubble diagram. Numerically, with $H_0 \cong 70$ Hubble units (H.u. hereafter) and $q_0 \cong -0.0605$ (see below), it follows

$$\gamma = 0^\circ \to \frac{\dot{r}_{obs}}{r} \cong H \cong 57 \text{ (H.u)} \tag{10}$$

$$\gamma = 180^\circ \to \frac{\dot{r}_{obs}}{r} \cong H \cong 83 \text{ (H.u.)} \tag{11}$$

4.7 Quick derivation of $\dot{r} = cz$

In the ECM the observed light space distance r at present time t_0, of a source emitting at the past epoch t_e, is given by the simple formula

$$r = -c \cdot (t_e - t_0) \tag{12}$$

Deriving eq. (12) with respect to t_e, if the positions

$$dt_e = 1/\nu_e = \lambda_e/c \qquad\qquad dt_0 = 1/\nu_0 = \lambda_0/c \tag{13}$$

hold good, where ν_e and ν_0 are the emitted and observed frequencies, it results

$$\dot{r} = \frac{dr}{dt_e} = -c \cdot \left(1 - \frac{dt_0}{dt_e}\right) = c \cdot \frac{\Delta\lambda}{\lambda_e} = cz \tag{14}$$

4.8 ECM solution of the nearby Universe from S&T data

The best values for H_0 and R_0 have been obtained from the solution of eq. (7) applied to the sample of 83 individual nearby galaxies, listed by S&T (1975) in their Tables 2,3,4, with distances r obtained by calibration of galaxy luminosity classes from known H II region sizes. The final solution in Hubble units, after introducing $\dot{r}_{obs}$ according to eq. (14), is that of paper II, and here summarized in **Table 0**.

Table 0

$H_0 = 70 \pm 3$	$q_0 \cong -0.0605$	$R_0 \simeq 260$	$a_0 \simeq 12.66$

Note that recently the WMAP mission has furnished $H_0 = 71 \pm 4$ H.u.(Bennett et al., 2003).

4.9 The successful test on historic samples

Eq. (7) has been successfully tested on many samples of nearby galaxies/groups/clusters, at known distances. In particular the fittings of two separate samples by Aaronson et al. (1982-1986), the first of 308 nearby individual galaxies at average distance $\langle r \rangle \cong 16\ Mpc$ and the second of 10 clusters at $\langle r \rangle \cong 71\ Mpc$, have given coinciding solutions of H_0 and R_0. Such a result represents a very strong proof in favor of the ECM and, consequently, the existence of a cosmic expansion center.

4.10 Galaxy escaping forever

One of the most significant results of the ECM emerges from a mathematical simulation, which provides a rate of variation of the Milky Way Hubble "constant" to light space r. Such a result, from $\delta r = -c\delta t$, can be written in $c.g.s.$ units

$$\frac{dH_{MW}}{dt} = -3H_{MW}^2 \tag{15}$$

which after integration gives

$$\Delta t = t - t_0 = \frac{1}{3H} - \frac{1}{3H_0} \tag{16}$$

As the Galaxy Hubble law (2) gives a Milky Way recession velocity $\dot{R}_{MW} = 0$ for $H = 0$, the time required for the Galaxy to stop, results to be, from eq. (16), $\Delta t = \infty$. This means that our Galaxy, within the limits of the simulation represented by the $H's$ derivative (15), should flee forever from the cosmic expansion center.

4.11 A resulting cosmic density $\rho_0 \sim 10^{-28} g/cm^3$

On the grounds of the simulation result (15), deriving eq. (2) with respect to time as follows

$$\frac{d\dot{R}_{MW}}{dt} = R_{MW}\frac{dH_{MW}}{dt} + H_{MW}\frac{dR_{MW}}{dt} \tag{17}$$

we obtain quickly the *c.g.s.* deceleration formula of the Galaxy

$$\ddot{R}_{MW} = -2H_{MW}^2 R_{MW} \tag{18}$$

whose dynamic interpretation, according to

$$\ddot{R}_{MW} = -\frac{4}{3}\pi G\rho R_{MW} + \dot{\theta}_{MW}^2 R_{MW}, \tag{19}$$

leads to the following density formula

$$\rho_0 = \frac{3H_0^2(2+y_0^2)}{4\pi G_0} \tag{20}$$

where $\dot{\theta}_0 = y_0 H_0$. Eq. (20), putting $y_0 \simeq 2$ (Lorenzi, 2003a,2002) and $H_0 \cong 70$ H.u., gives numerically $\rho_0 \simeq 1.1 \times 10^{-28} g/cm^3$.

4.12 Universe as old as the Moon ?!

The (16) solution holds another fundamental result. In fact, putting $H = \infty$ at the time $t = 0$, our epoch t_0 results from the *c.g.s.* formula

$$t_0 = \frac{1}{3H_0} \tag{21}$$

that numerically, with $H_0 = 70 \pm 3\ Km\ s^{-1} Mpc^{-1}$, gives a Universe age $t_0 = 4.7 \pm 0.2$ Gyr, which is slightly greater than the atomic age of the oldest meteorites, $t_{meteor} = 4.53 \pm 0.02\ Gyr$, or the oldest lunar rock, $t_{moon} = 4.6 \pm 0.1\ Gyr$ (Allen's Ap. Q., 1999).

4.13 How small is the Universe !

Some considerations are now necessary about the observed size of the Universe. The starting point has to be the ECM eq. (7), which, being $H_0 r = cx/3$ and $\dot{r} = cz$ with $\dot{w} \equiv 0$ assumed, can be applied to any z in the form

$$z = \frac{x}{3}\left(\frac{1+x}{1-x}\right)\left[1 + 3q_0\frac{(1-x)^{1/3}}{1+x}\cos\gamma\right] \tag{22}$$

A quick discussion of the algebric sign of eq. (22) gives the following result

$$z > 0 \Rightarrow x < 1 \Rightarrow r < \frac{c}{3H_0} \tag{23}$$

whose significance seems to prospect a very embarrassing situation. In fact, within the limits of the ECM in the present form, we are obliged to conclude that the observed Universe is very small. On the other hand such a conclusion is the natural consequence of the reduced age t_0, according to eq. (21).

5. Further Developments Of The ECM

5.1 The Hubble law by Sandage (1972)

Allan Sandage (1972) obtained one of his historical results with an accurate verification of the fitting linear law in H.u.

$$cz = H_0 D_L \tag{24}$$

by studying the Hubble diagram of the brightest galaxies of 82 clusters, in the observed range of $z \lesssim 0.33$. The method used by Sandage was the $m - z$ relation, based on the classical luminous distance D_L in megaparsecs, defined by

$$\log D_L = 0.2(m - M) - 5 \tag{25}$$

where the absolute magnitude M is considered a constant unknown (like H_0), equal for all the 82 brightest galaxies, and m is the observed magnitude. In the attempt to write the ECM equation (7) according to formulation (24), after applying $\dot{r}_{obs} = cz$ (eq. (14)) it is best to rewrite eq. (7), where $a_0 = -3H_0 q_0$, as follows

$$cz = H_0 r \cdot \left(\frac{1+x}{1-x}\right)\left[1 + 3q_0 \frac{(1-x)^{1/3}}{1+x}\cos\gamma\right] \tag{26}$$

which can be written

$$cz = H_0 D_z \qquad with \qquad D_z = r \cdot \left(\frac{1+x}{1-x}\right)\left[1 + 3q_0 \frac{(1-x)^{1/3}}{1+x}\cos\gamma\right] \tag{27}$$

Consequently, by force of the verified eq. (24), the Sandage luminous distance D_L would have to satisfy the equality $D_L = D_z$.

Indeed the experimental evidence for wedge-shaped Hubble diagrams and ECM dipoles of the nearby Universe, based on luminous distances, firmly gives $D_L \neq D_z$. Hence, we must conclude that either the ECM is erratic or the Sandage result (24) needs some explanation.

5.2 The RFR effect analysis (1973)

Rubin, Ford and Rubin (1973)(RFR hereafter) obtained a different result from the above found by Sandage. Using the same method, however applied to ScI galaxies with $14.0 \leq m \leq 15.0$, at redshift $z \lesssim 0.033$, they found

$$cz = H_i \cdot D_L \tag{28}$$

with

$$H_1 = 72 \pm 4 \text{ (Region 1)} \qquad H_2 = 93 \pm 4 \text{ (Region 2)} \tag{29}$$

where H_1 and H_2 are the observed values of H in two different Regions of the sky. If again one wishes to concile the ECM equation (26) with the RFR result (28)(29), we are obliged to consider solutions based on some equalities, such as those listed below as examples:

$$H_i = H_0 \cdot \left[1 + 3q_0 \frac{(1-x)^{1/3}}{1+x} \cos\gamma\right] \qquad D_L = r \cdot \left(\frac{1+x}{1-x}\right) \tag{30}$$

Therefore one can conclude that good compatibility exists between the RFR effect and the ECM.

5.3 The Perlmutter group result by SNe Ia (1999)

Within the Supernova Cosmology Project (SCP hereafter), the Perlmutter group announced another sensational result (Perlmutter et.al. 1999), which again is different from that found by Sandage. Using the same method, based on a constant absolute magnitude and here applied to 42 high-redshift Type Ia supernovae discovered by the SCP, at redshifts z between 0.18 and 0.83, and 18 low-redshift Type Ia supernovae from Calan/Tololo Supernova Survey (Hamuy et al. 1996), at redshifts z below 0.1, the Perlmutter group obtained a fitted Hubble diagramm in the $m - z$ form, that can be approximately described by the empirical law

$$cz \cdot (1+z) = H_0 D_L \tag{31}$$

Also such a SCP result (31) does not agree with the ECM at first sight, as it excludes any dipole anisotropy of the Hubble ratio between two observed quantities, as are z and the luminous distance D_L.

5.4 Search for an algorithm based on fictitious luminous distances

All the above results, by Sandage, by RFR, and by the SCP, seem indeed to prospect a very intricate and ambiguous situation. In order to get round such an impasse, an attempt has been carried out by means of a mathematical algorithm to combine in a single expression the ECM and the results of Sandage, RFR, and SCP above all. That is considering D_L of (24) or (31) as a fictitious luminous distance D_{FL} in the form

$$D_{FL} = r \cdot (1+z)^n \cdot \left(\frac{1+x}{1-x}\right) \tag{32}$$

Now, the ECM eq. (26) can be transformed into a fac-simile of the empirical law (31)

$$cz \cdot (1+z)^n = H_0 D_{FL} \left[1 + 3q_0 \frac{(1-x)^{1/3}}{1+x} \cos\gamma\right] \tag{33}$$

The previous formula with $n = 0$ and $n = +1$ represents two equations which still differ from the empirical laws by Sandage and SCP by the factor in square brackets. But such a factor in eq. (33), differently from eq. (7), has an angular coefficient decreasing with distance; hence it clearly produces the effect of reducing the wedge amplitude of the Hubble diagram with distance, giving just eq. (24) or (31) as mathematical limit result for $x \to 1$, that is for $r \to \frac{c}{3H_0}$. Note that the fictitious luminous distance D_{FL} has a true experimental value, as it results from the observed magnitude m, according to eq. (25). At the same time D_{FL} depends on a fictitious absolute magnitude M, which will be true only if it maintains a constant value in the $m - z$ relation for sources all having the same intrinsic luminosity. Reversely M is closely connected to D_{FL}, that is to the value assumed by n in eq. (32), according to eq. (25) written as follows

$$M = m - 5\log D_{FL} - 25 \tag{34}$$

In conclusion, we might rewrite eq. (33) in terms of a practical formulation of dipole, that finally results to be

$$\frac{cz \cdot (1+z)^n}{D_{FL}} = H_0 - a_0 \frac{(1-x)^{1/3}}{1+x} \cos\gamma \tag{35}$$

5.5 Dipole test on remote rich clusters

Referring to sources all assumed as having the same absolute magnitude within the sample, the practical check of eq. (35) still has a problem, that of the variable x

included into the angular coefficient. To get over such a difficulty, we should choose a dipole type equation, as the following

$$\frac{cz \cdot (1+z)^n}{D_{FL}} = H_0 - a^*(x) \cdot \cos\gamma \tag{36}$$

where $x = 3H_0 r/c$ should remain practically unchanged, to give a constant $a^*(x)$, and M is chosen in order to give fictitious luminous distances D_{FL} able to confirm the expected value of H_0. That means to restrict the field of application of eq. (36) to a sample of data having a very restricted range of distances r. Being r unknown, a choice, although non rigorous, may be that of considering restricted ranges of the observed magnitude m. Curiously such a useful procedure is like that followed in 1973 by Rubin, Ford and Rubin ! So it will be very interesting to carry out its verification on samples of remote clusters. Chiefly such a check has been done on the homogeneous and concentrated sample of 66 clusters of Richness 3, those having a z value in the Abell catalogue (Abell, Corwin, Olowin, 1989), and here listed in **Table A** of the Appendix. The dipole test on different ranges of magnitude m_{10} of the tenth brightest cluster member in Abell's system, with the n values suggested by the SCP and Sandage solutions respectively, has been carried out on 7 key range-samples, for a total of 61 clusters having magnitudes m_{10} between the values of 16.9 and 18.0. The magnitude ranges have all been fixed at half magnitude. Concerning this dipole test we must still remark an obvious but very important condition to take into account: it always needs a sufficiently rich and homogeneous distribution of sample members over the two hemispheres of the expansion direction, in order to guarantee the best statistical significance of the fitting solution.

The main features of the 7 key samples, numbered IV-V-VI-VII-VIII-IX-X respectively, plus the whole samples I-II-III from the Abell catalogue (Abell, Corwin, Olowin, 1989) and the two sub-samples IIINear and IIIFar, are compared in **Table 1**, where the following data is listed in order: sample ordinal number; cluster richness Ri; magnitude range of m_{10}; number N of sample clusters; unweighed mathematical mean $\langle m_{10} \rangle$ of the magnitudes m_{10} of the Abell clusters of Richness Ri with z tabled; unweighed mathematical mean $\langle z \rangle$ of the corresponding redshifts; inferred value of the sample distance $r_{\langle z \rangle}$ in Mpc from the numerical x solution of the ECM equation (22) with $z = \langle z \rangle$ and $\cos\gamma = 0$ assumed, having $r_{\langle z \rangle} = cx/3H_0$ and $H_0 = 70$ H.u. adopted.

Table 1

Sample	Ri	magnitude range	N	$\langle m_{10}\rangle$	$\langle z\rangle$	$r_{\langle z\rangle}$
I	1	$12.7 \leq m_{10} \leq 18.4$	246	16.46	0.1006	286.7
II	2	$12.5 \leq m_{10} \leq 18.0$	128	16.83	0.1319	345.0
III	3	$15.0 \leq m_{10} \leq 18.0$	66	17.283	0.1739	411.5
IIINear	3	$m_{10} \leq 17.4$	37	16.981	0.1469	370.1
IIIFar	3	$m_{10} \geq 17.4$	39	17.600	0.2087	458.9
IV	3	$16.9 \leq m_{10} \leq 17.4$	32	17.197	0.1592	389.5
V	3	$17.0 \leq m_{10} \leq 17.5$	36	17.264	0.1623	394.3
VI	3	$17.1 \leq m_{10} \leq 17.6$	41	17.393	0.1800	420.3
VII	3	$17.2 \leq m_{10} \leq 17.7$	39	17.454	0.1896	433.6
VIII	3	$17.3 \leq m_{10} \leq 17.8$	38	17.555	0.2027	451.2
IX	3	$17.4 \leq m_{10} \leq 17.9$	37	17.578	0.2054	454.7
X	3	$17.5 \leq m_{10} \leq 18.0$	29	17.669	0.2084	458.6

The obtained results of the unweighed fitting of eq. (36) with $n = +1$ and $n = 0$ by turns, through the least square method, applied firstly to the whole Sample III for comparison and hence to all 7 range-samples IV-V-VI-VII-VIII-IX-X, are listed in **Table 2**. Here the 8 columns report in order the following data and results: sample ordinal number; number N of sample clusters; adopted value of n; expected value a^*_{ECM} of the angular coefficient $a^*(x)$ of eq. (36) for the range-samples, being $x = 3H_0 r_{\langle z\rangle}/c$ and $a_0 = -3q_0H_0$ with $H_0 = 70$ H.u. and $q_0 = -0.0605$ H.u. adopted; absolute magnitude M_d in Abell's system, confirming the expected value of H_0 in the dipole fitting; standard deviation s in H.u. of the fitting; resulting H_0 from the fitting in its forced coincidence with the adopted 70 H.u.; resulting angular coefficient a^* in H.u. from the fitting.

Table 2

Sample	N	n	a^*_{ECM}	M_d	s	H_0	a^*
III	66	+1		-22.354	20.8	70.0 ± 2.6	$+2.2 \pm 4.2$
IV	32	+1	+9.0	-22.309	24.6	70.0 ± 4.5	$+4.5 \pm 6.7$
V	36	+1	+8.9	-22.313	23.4	70.0 ± 4.1	$+6.1 \pm 6.1$
VI	41	+1	+8.7	-22.451	19.7	70.0 ± 3.2	$+8.2 \pm 4.9$
VII	39	+1	+8.6	-22.521	19.8	70.0 ± 3.3	$+8.2 \pm 5.1$
VIII	38	+1	+8.5	-22.584	18.2	70.0 ± 3.1	$+7.8 \pm 5.0$
IX	37	+1	+8.5	-22.581	18.3	70.0 ± 3.1	$+6.1 \pm 4.9$
X	29	+1	+8.4	-22.488	14.7	70.0 ± 2.8	-1.4 ± 4.6
III	66	0		-21.981	17.4	70.0 ± 2.2	$+1.9 \pm 3.5$
IV	32	0	+9.0	-21.954	20.7	70.0 ± 3.8	$+3.1 \pm 5.6$
V	36	0	+8.9	-21.952	19.8	70.0 ± 3.5	$+4.6 \pm 5.2$
VI	41	0	+8.7	-22.062	16.7	70.0 ± 2.7	$+6.5 \pm 4.1$
VII	39	0	+8.6	-22.116	16.7	70.0 ± 2.8	$+6.7 \pm 4.3$
VIII	38	0	+8.5	-22.160	15.4	70.0 ± 2.6	$+6.5 \pm 4.2$
IX	37	0	+8.5	-22.156	15.5	70.0 ± 2.6	$+5.0 \pm 4.2$
X	29	0	+8.4	-22.067	12.3	70.0 ± 2.4	-0.9 ± 3.9

Among the data listed in **Table 2** one can observe better fittings at $n = 0$, accompanied by slowly variable absolute magnitudes M_d, however with too small angular coefficients a^*. At the same time the seemingly worst solution at $n = +1$ presents angular coefficients a^* nearer to the expected a^*_{ECM} for the ECM dipole, and higher absolute magnitudes clearly increasing with distance. So this dipole test on remote rich clusters seems to speak in favor of eq. (32) with $n = +1$, that is the SCP result, and at the same time it suggests that an empirical relation of M with distance should be sought.

5.5.1 Absolute magnitudes increasing with square distance

If the ECM equation (7) holds good in the form (22), it is possible to obtain (by trial and error) the r value which strictly confirms the z eq. (22) for each cluster of Sample III, through the nearby solution of **Table 0** and data listed in **Table A** of the Appendix. Note how these values of r, here called r_z and listed in column 7 of **Table A**, are identical both for $n = +1$ and $n = 0$. At this point, after obtaining from eq. (34) the absolute magnitude M of each tenth brightest cluster member according to eq. (32)

$$M_1 = m_{10} - 5\log\left(r_z \cdot (1+z)^n \cdot \frac{1+x}{1-x}\right) - 25 \tag{37}$$

or, alternatively, in the form based on luminous distances from eqs. (24) and (31), as

$$M_2 = m_{10} - 5\log(cz(1+z)^n/H_0) - 25 \tag{38}$$

the empirical relation to check is the following MacLaurin formula

$$M = M_0 + r_z \cdot \left(\frac{dM}{dr_z}\right)_0 + \frac{r_z^2}{2}\left(\frac{d^2M}{dr_z^2}\right)_0 \tag{39}$$

which can now be solved through the least squares method. The related four fittings of M_1 and M_2, with $n = +1, 0$ by turns, have been carried out on all the 66 clusters of Sample III, whose magnitudes $M_1(n = +1)$, listed in column 8 of **Table A** of the Appendix, are plotted against r_z in **Figure 1**. The fitting results which stem from the adoption of eq. (39) have been listed in **Table 3**, where the 2^{nd} order solution follows after fixing $(dM/dr_z)_0 \equiv 0$, having verified its negligibility.

Table 3

2^{nd} order	N	n	M_0	$\left(\frac{dM}{dr_z}\right)_0$	$\left(\frac{d^2M}{dr_z^2}\right)_0$	s
M_1	66	+1	-20.866 ± 0.084	0	$-1.644 \pm 0.089 \times 10^{-5}$	0.2632
M_2	66	+1	-20.908 ± 0.098	0	$-1.553 \pm 0.104 \times 10^{-5}$	0.3073
M_1	66	0	-20.782 ± 0.084	0	$-1.342 \pm 0.090 \times 10^{-5}$	0.2659
M_2	66	0	-20.825 ± 0.094	0	$-1.251 \pm 0.100 \times 10^{-5}$	0.2960

The solutions reported in **Table 3** give the absolute magnitude M increasing with square distance; furthermore the standard deviations s show that the M_1 expression of eq. (37) clearly improves the fittings, confirming the RFR effect against the Hubble law (24) represented by eq. (38) with $n = 0$, and also that $n = +1$ in eq. (37) is slightly better than $n = 0$. Consequently, such a ECM test speaks in favor of the M_1 of eq. (37), and thus the luminous distance (32).

5.5.2 Final dipole test in favor of $n = +1$

Eq. (37), putting M_1 equal to eq. (39) with known coefficients, makes it possible to test again the ECM dipole. To this end the two M_1 quadratic solutions of **Table 3** are adopted. The values of D_L, for each value of r_z and $n = +1$ and $n = 0$ respectively, follow from eq. (25) in the form

$$D_L = 10^{0.2\left[m_{10} - M_0 - \frac{r_z^2}{2}\cdot\left(\frac{d^2M}{dr_z^2}\right)_0\right]-5} \tag{40}$$

Therefore it is now possible to carry out a new fitting of the dipole equation (36), that this time can be rewritten as

$$\frac{cz(1+z)^n}{D_L} = H_0 - a_0 \cdot X \tag{41}$$

where

$$X = \frac{(1-x)^{1/3}}{1+x}\cos\gamma \tag{42}$$

is a computable function of $\cos\gamma$ and x for each cluster ($x = 3H_0 r_z/c$ with $H_0 = 70$ H.u. adopted). In this way each of the 66 clusters of Sample III has its ratio $cz(1+z)^n/D_L$, for $n = +1$ and $n = 0$ respectively. Of course such a new test is specifically addressed to verifying the value of a_0, which comes from the adopted value of n. Because the function X of eq. (42) is now known, the new test of eq. (41) can be meaningfully applied to the whole Sample III, and to the sub-samples, IIINear and IIIFar, as a further verification. The results of such a least squares unweighed fitting are listed in **Table 4**. Here the columns report in order the following data: sample ordinal number; number N of clusters; average distance $\langle r_z \rangle$ of the sample; adopted values of n; standard deviation s in H.u. of the fitting; resulting H_0 in H.u. from the fitting; resulting angular coefficient a_0 in H.u. from the fitting.

Table 4

Sample	N	n	$\langle r_z \rangle$	s	H_0	a_0
III	66	+1	404.63	8.81	70.40 ± 1.10	$+11.85 \pm 2.48$
IIINear	37	+1	361.65	9.84	74.17 ± 1.64	$+12.29 \pm 3.47$
IIIFar	39	+1	458.79	5.70	67.85 ± 0.93	$+12.42 \pm 2.26$
III	66	0	404.63	8.83	70.24 ± 1.11	$+10.16 \pm 2.48$
IIINear	37	0	361.65	9.82	74.07 ± 1.63	$+10.73 \pm 3.46$
IIIFar	39	0	458.79	5.56	67.54 ± 0.91	$+10.32 \pm 2.20$

Table 4 clearly confirms that $n = +1$ is more consistent than $n = 0$ with the solution of **Table 0**, referring to the nearby Universe. In conclusion, **Figure 2** shows the plot of $cz(1 + z)/D_L$ against $-X$ (listed in column 10 and 9 of **Table A** in Appendix**,** respectively), corresponding to the $n = +1$ solution of Sample III in **Table 4.**

5.6 An empirical formula for the cosmological luminous distance D_C

Note that any n solution of eq. (33) means multiplying by the same factor $(1+z)^n$ the first and second members of the ECM eq. (26), which consequently remains unchanged. The difference arises when we assemble the expression of the luminous distance D_{FL}, according to eq. (32). In fact, such a D_{FL} with $n = +1$, as well as confirming the ECM dipole of clusters, is able to maintain the constant absolute magnitude of the supernovae SNe Ia, according to the SCP result (31). Hence, if we must accept the good standard candle of the supernovae SNe Ia, as is generally recognized by the astronomical community (Willick, 1999), D_{FL} with $n = +1$ must represent a true, non fictitious, cosmological luminous distance D_C.

Instead, in the case of the 7 key cluster samples, the value of n able to mantain the constancy of the absolute magnitude of the tenth brightest cluster member is $n < 0$; therefore, if we consider the brightest cluster galaxies (BCGs) as good candles, the true luminous distance should be D_{FL} with $n < 0$, with the paradox, always according to the ECM, of having supernovae intrinsically much fainter at higher redshifts z.

In conclusion the important result of the SCP on SNe Ia seems to suggest both the agreement with the ECM and, as a further and important consequence, an empirical formulation of the cosmological luminous distance D_C, which results to be the same as eq. (32) with $n = +1$, as a function of two variables, the cosmologic redshift z and the light space distance r, and of two constants, the Hubble constant H_0 at our epoch t_0 and the light speed c in space.

6. A Comparative Outline Of 3 Historical Models

What has been presented in the previous sections seems to outline a cosmological scenario very different from that which is called the standard cosmological model. Nevertheless the apparently revolutionary results of the ECM about the age and structure of the Universe are not completely new. Warning signs of these results were already present in three historic models developed by Einstein, de Sitter, Lemaitre, Dirac, Gamow, at the beginning of modern cosmology.

6.1 The Einstein-de Sitter Model (1932)

A concise version of the Einstein-de Sitter model (EDSM hereafter) may be easily presented within Newtonian cosmology, with a few links to the ECM. If we consider the scale factor R as coinciding with the distance R_{MW} of the Galaxy from the void center VC, the rate of variation of H with respect to time, in $c.g.s.$ units, may be drawn from the derivative with respect to time of the Galaxy Hubble law (2) according to eq. (17); so it results to be

$$\frac{dH}{dt} = \frac{\ddot{R}}{R} - H^2 \tag{43}$$

where

$$\frac{\ddot{R}}{R} = -\frac{GM}{R^3} + \dot{\theta}^2 \tag{44}$$

The eq. (44), using the total energy expression of a unitary mass having velocity $v = (\dot{R}^2 + R^2\dot{\theta}^2)^{1/2}$ in the form

$$\frac{1}{2}(\dot{R}^2 + R^2\dot{\theta}^2) - \frac{GM}{R} = K \tag{45}$$

can be rewritten, with $\dot{R} = HR$, as

$$\frac{\ddot{R}}{R} = \frac{K}{R^2} - \frac{H^2}{2} + \frac{\dot{\theta}^2}{2} \tag{46}$$

Hence the $H's$ derivative (43), after the introduction of eq. (46), becomes

$$\frac{dH}{dt} = -\frac{3}{2}H^2 + \frac{\dot{\theta}^2}{2} + \frac{K}{R^2} \tag{47}$$

The Einstein-de Sitter model (1932) represents a special case of the above general formulation; it assumes the energy conservation law with $K = 0$, at the same time excluding the presence of any rotation, which signifies setting $\dot{\theta} = 0$. The consequent eq. (47), both when inserted into eq. (43) and when integrated alone with $H = \infty$ at $t = 0$, is able to furnish the most important output data of the EDSM, which is the matter density $\rho_0 = 3M/4\pi R_0^3$ and the age of the Universe t_0, as

$$\text{EDSM:} \qquad \rho_0 = \frac{3H_0^2}{8\pi G} \qquad t_0 = \frac{2}{3H_0} \tag{48}$$

Note that the previous solution is strictly based on the constant zero value of K, with $\dot{\theta} = 0$.

Now it is possible to test the general eq. (47) after adopting the ECM result of eq. (15) and the consequent (18) formula for $\ddot{R}$. In this case the eq. (47), by introducing $dH/dt = -3H^2$, gives

$$\frac{\dot{\theta}^2}{2} + \frac{K}{R^2} = -\frac{3}{2}H^2 \tag{49}$$

which, through the $\dot{\theta}^2$ expression from eq. (44) with $\ddot{R} = -2H^2R$, can be written more explicitly as the conclusive ECM result, in the form

$$\text{ECM:} \qquad K = -\frac{\dot{R}^2}{2} - \frac{GM}{2R} \tag{50}$$

Consequently the ECM, by comparison with the EDSM and other models, does not agree with the conservation law of mechanical energy, when the energy is computed within a single Newtonian cosmic space reference. Reversely, as the energy conservation law for an isolated system must be respected, it should be the gravitational reference to rotate, following in some way the cosmic matter in its flight from the expansion center. In other words, the transverse velocity of our Galaxy from eq. (49), as

$$\dot{\theta}R = (-3\dot{R}^2 - 2K)^{1/2} \tag{51}$$

, should be considered as referred to a gravitational reference system rotating with angular velocity $-\dot{\theta}$ with respect to the radial direction.

In conclusion, it seems possible to conciliate the ECM with the energy conservation law only by assuming some kind of dragging of cosmic gravitational references.

6.2 The Dirac (1937-38) theory of Large Numbers Hypothesis

The Dirac theory of Large Numbers Hypothesis (LNH; Dirac 1937-38) bases itself on the fundamental hypothesis of direct proportionality between the Hubble and the

universal gravitation constants, that is $G \propto H$, when dealing with the density formula derived from classical mechanics. It has been shown in a previous paper (Lorenzi, 2002) the accordance with the ECM, essentially expressed by the following age result in *c.g.s.* units

$$\text{LNH:} \qquad t_0 = \frac{1}{3H_0} \tag{52}$$

Here we will try to proceed in the opposite direction, that is starting from the ECM to verify its compatibility with the LNH. The Galaxy dynamic equation (19), now written as

$$\frac{4}{3}\pi\rho G = 2H^2 + \dot{\theta}^2, \tag{53}$$

represents our only hypothesis, of course in the ECM context. After putting $\dot{\theta} = yH$, and taking into account the ECM results $\rho = \rho_0 t_0/t$ and $H = H_0 t_0/t$ (Lorenzi, 2002), eq. (53) leads to

$$\frac{\rho}{H} = \frac{3H(2+y^2)}{4\pi G} = \frac{\rho_0}{H_0} = \text{constant} \tag{54}$$

from which we can conclude that the ECM must necessarily lead to the proportionality

$$G \propto H \cdot (2+y^2). \tag{55}$$

The Dirac theory simply coincides with $y = 0$, while the ECM considers a $\dot{\theta}$ value, probably with $y_0 \simeq 2$, referring to the likely rotation of the Universe at our epoch t_0 (cf. Lorenzi, 2003a, 2002).

6.3 The Historic Big Bang Model

The Big Bang model is more properly a physical than astronomical subject. However it deals with a few fundamental cosmic parameters, whose measurements is possible through observational cosmology. Among these we cite again the density matter and the age of the Universe. The values inferred from the ECM for ρ_0 and t_0 are higher and smaller respectively, with respect to those normally accepted within the standard model, which is based, it is well to remember, on general relativity. Here, without entering into details of the Big Bang physical model, an attempt in qualitative terms will be made to show briefly some possible assonances between the ECM results and a few aspects of the work of Big Bang founders, such as Lemaitre and Gamow.

6.3.1 The Lemaitre Primeval Atom (1931)

The first scientist to consider the origin of the Universe as a big explosion was the belgian abbot Georges Lemaitre (1931, 1946) (Merleau-Ponty, 1965). He hypothesized the primordial explosion as being caused by a sort of fission cosmic bomb, whose fragments started the journey producing the present expansion of the Universe. This was his first idea, soon abandoned in favor of the relativistic models, but later taken again into account through the so-called "primeval atom". According to such a speculative model the "protogalaxies" should have come out of extremely small concentrated bodies, which were simply the splinters of that primeval atom. What are the remnants of these primordial splinters in the observed Universe? An answer to such a question might be referred to the unknown origin of the active galactic nuclei, the so-called AGN, whose definition in terms of huge galactic black holes is surely as correct as the large holes in our understanding and knowledge of their nature and physical structure. This reference to the AGN, and then to all the galaxies as evolving structures of primeval atom remnants, is only linked to the introductory toy-model (Lorenzi, 1999a) of the ECM, which represents an extremely simplified attempt to describe a Hot Hard Big Bang according to the Lemaitre primeval atom hypothesis.

6.3.2 Regarding the Gamow Physical Model (1948)

Seemingly one of the biggest obstacles to the acceptance of the ECM is the age result. Indeed, apart from the Dirac theory, almost all the scientific literature seems to consider only higher ages, as $t_0 = 1/3H_0$ is too small if compared to the nuclear timescales for stellar evolution theory, which does not depend upon the assumption that G varies with time. The close tie between stellar evolution and nucleosynthesis is strictly due to the rejection of Gamow's early result (Gamow, 1948)(Alpher & Herman, 1948) of the cosmological nucleosynthesis of all the elements, which in his theory were produced by Big Bang after a rapid process of neutron addition. Primordial nucleosyntheis was finally accepted only for Helium and a few isotopes, but not for heavy elements. At this point, if we accept both the primordial Helium origin and an Universe age very near to that of the oldest meteorites or lunar rochs, Gamow's mechanism of nucleosyntheis of heavy elements should be at least re-examined, under state-equations able to reproduce the observed abundances. At present there is one important observation which might be interpreted according to the primordial origin of the elements. That is the X-ray gas ($T \simeq 10^8 K$) in the intergalactic medium (IGM) in rich clusters, showing quite high metal abundances (Mitchell et al., 1976) and with a total mass in the order of that of the same cluster. Perhaps much of the cluster gas is stripped from the cluster galaxies, but its origin may have only two possible explanations: one is related to frequent supernova explosions in the young Universe, the other necessarily refers

to the primordial IGM. The observed diffuse X-ray background is certainly strongly contributed to by IGM. So, as well as the cosmic microwave background at $T \cong 2.7$ K (Penzias & Wilson, 1965), the X-ray background might also be closely tied to the very early Universe.

7. Conclusion

After so much analysis and discussion of data, results and models, the best conclusion is that it is better to draw no conclusion. In fact the empirical expansion center model is opening problems rather than closing them. The check work has to go on. Likely corrections will be necessary in future; and some mistakes may be found. However, one feature will certainly survive. That is the reality of the expansion center! The next appointment will be with further SNe Ia tests, specifically addressed to monitor their respect of the dipole equation. Furthermore the cosmic background radiation shall be deeply analysed in the same context.

8. Acknowledgments

The author wishes to thank Prof. Cesare Barbieri for his useful comments after reading the manuscript, and M. Nonino with the meeting Editors L. Girardi and S. Zaggia for all their help.

References

Aaronson, M. et al. 1982, Ap. J. Suppl. Series, 50, 241

Aaronson, M. et al. 1986, Ap. J. 302, 536

Abell, G.O., Corwin, H.G., Olowin, R.P. 1989, Ap. J. Suppl. Series, 70, 1

Alpher, R. A. and Herman, R. C. 1948, Nature 162, 774

Bahcall, N.A. 1988, Ann. Rev. Astron. Astrophys. 26, 631

Bahcall, N.A. and Soneira, R.M. 1982, Ap. J. 262, 419

Bennett, C. L. et al. 2003, ApJS 148, 1

Chaisson, E.J. 1990, Glossary for HST (Space Telescope Science Institute, Baltimore, Maryland)

Cox, A.N. 1999, Allen's Astrophysical Quantities (AIP Press, Springer)

de Vaucouleurs, G. 1965, in "Galaxies and the Universe", 1975, Vol. IX of Stars and Stellar Systems, p. 566, The University of Chicago Press

Dirac, P.A.M. 1937, Nature 139, 323

Dirac, P.A.M. 1938, RSPSA, 165, 199

Einstein, A., and de Sitter, W. 1932, Proc. N.A.S. 18, 213

Gamow, G. 1948, Nature 162, 680

Geller, M.J. and Huchra, J.P. 1989, Science 246, 897

Hamuy, M., et al. 1996, AJ, 112, 2391

Kirshner,R.P., Oemler, A., Jr., Schechter, P.L.and Schectman, S.A. 1981, Ap.J., 248, L57

Lahav, O. 1987, Mon. Not. R. astr. Soc. 225, 213

Lemaître, G. 1931, in Couderc, P. 1933, Discussions sur l'évolution de l'Universe, Gauthier-Villars

Lemaître, G. 1946, L'Hypothèse de l'atom primitif, Neuchatel, Griffon

Lorenzi, L. 1989, 1991, Contributi N. 0,1, Centro Studi Astronomia-Mondovì, Italy

Lorenzi, L. 1995bc, Sesto Pusteria International Workshop Book, eds.-SISSA ref. 65/95/A

Lorenzi, L. 1994, in 1996, Astro. Lett. & Comm., 33, 143 (Grado3 Proc., eds.-SISSA ref. 155/94/A)

Lorenzi, L. 1999a, in 2000 MemSAIt, 71, 1163 (reprinted in 2003, MemSAIt, 74)

Lorenzi, L. 1999b, in 2000 MemSAIt, 71, 1183 (reprinted in 2003, MemSAIt, 74)

Lorenzi, L. 2002, in 2003, MemSAIt, 74, 480, (see also the poster paper on line)

Lorenzi, L. 2003a, (parallel paper)

Mitchell, R. J. et al. 1976, MNRAS, 176, 29P
Meiksin, A. & Davis, M., 1986, Astr. J., 91, 191
Merleau-Ponty J. 1965, Cosmologie du XX Siecle, Editions Gallimard
Nottale, L., Pecker, J.C., Vigier, J.P., et Yourgrau, W. 1976, La Recherce 68, V. 7, 529
Penzias, A.A., and Wilson, R.W. 1965, Ap. J., 142, 419
Perlmutter, S., et al. 1999, Ap. J. 517, 565
Rowan-Robinson,, M. 1988, Space Science Review 48,1
Rubin, V.C., Ford, W.K., and Rubin, J.S. 1973, Ap. J. Letters 183, L111 (RFR)
Sandage, A. 1972, Ap. J. 178,1
Sandage, A. and Tammann, G.A. 1975, Ap. J. 196, 313 (Paper V)
Willick, J.A. 1999, in "Formation of Structure in the Universe" (Cambridge University Press)
Yahil, A., Walker, D., Rowan-Robinson, M. 1986, Ap. J. 301, L1

FIGURES

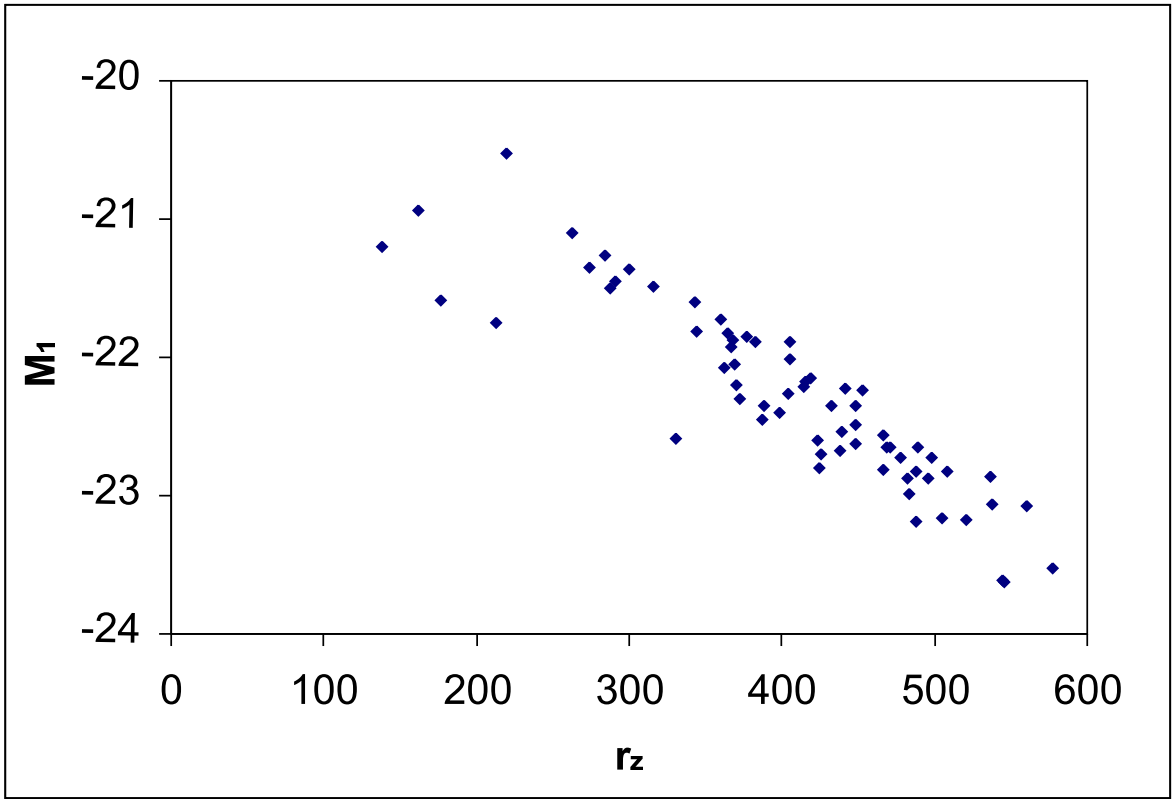

Figure 1: Plot of the absolute magnitude $M_1 = m_{10} - 5\log\left(r_z \cdot (1+z) \cdot \frac{1+x}{1-x}\right) - 25$ against the distance r_z in Mpc, for each cluster of Sample III

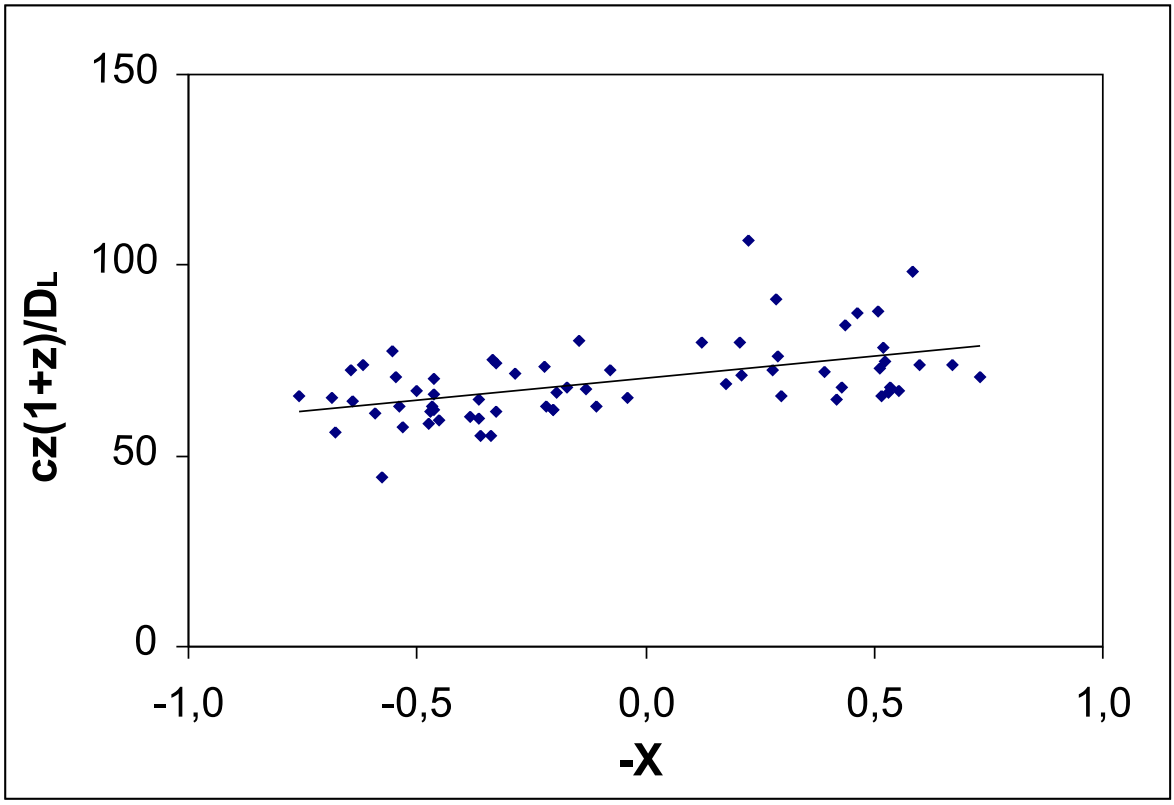

Figure 2: Plot of $cz(1+z)/D_L$ against $-X$, for each cluster of Sample III

APPENDIX

Table A1

Cluster	l	b	$-\cos\gamma$	z	m_{10}	r_z	$M_{1_{n=+1}}$	$-X$	$\frac{cz(1+z)}{D_L}$
A0022	42.89	−82.98	+0.72072	0.1432	17.5	342.79	−21.529	−0.5303	66.8
A0041	113.22	−54.60	+0.46051	0.275	17.6	520.76	−23.171	−0.2901	76.3
A0042	65.76	−83.78	+0.69151	0.1087	17.1	283.63	−21.262	−0.5358	68.0
A0098	121.36	−42.37	+0.27377	0.105	16.9	287.77	−21.500	−0.2114	71.1
A0115	124.21	−36.54	+0.18020	0.1971	17.3	438.04	−22.675	−0.1220	79.6
A0140	166.69	−85.67	+0.59003	0.152	17.5	360.51	−21.713	−0.4275	68.1
A0141	175.32	−85.93	+0.58997	0.230	17.7	466.68	−22.568	−0.3897	72.0
A0209	159.88	−73.47	+0.43795	0.206	17.8	441.65	−22.221	−0.2956	65.8
A0222	162.47	−72.22	+0.41486	0.211	17.6	448.75	−22.489	−0.2783	72.4
A0223	62.42	−71.99	+0.77155	0.207	17.6	432.81	−22.349	−0.5249	74.7
A0274	161.58	−64.29	+0.30178	0.1289	16.3	330.84	−22.586	−0.2244	106.3
A0520	195.81	−24.28	−0.43390	0.203	17.4	465.85	−22.814	+0.2868	71.5
A0586	187.54	+21.93	−0.94466	0.171	17.4	438.87	−22.534	+0.6393	64.3
A0593	142.22	+30.28	−0.72426	0.226	17.4	504.68	−23.162	+0.4627	70.4
A0639	147.56	+33.27	−0.78582	0.291	17.7	577.62	−23.527	+0.4707	61.6
A0655	172.68	+35.13	−0.94945	0.1245	17.1	362.45	−22.078	+0.6868	65.1
A0750	218.77	+35.52	−0.94405	0.162	17.1	425.24	−22.703	+0.6465	72.6
A0795	217.09	+40.14	−0.95701	0.1357	17.5	382.69	−21.884	+0.6801	56.3
A0868	244.72	+32.49	−0.76302	0.153	17.6	404.82	−22.012	+0.5319	57.6
A0873	139.90	+39.41	−0.74672	0.182	17.4	447.91	−22.629	+0.5013	67.1
A0963	182.62	+55.86	−0.95194	0.206	17.2	487.63	−23.193	+0.6173	73.8
A1246	224.14	+69.27	−0.83801	0.216	17.6	496.35	−22.879	+0.5393	62.8

Table A2

Cluster	l	b	$-\cos\gamma$	z	m_{10}	r_z	$M_{1_{n=+1}}$	$-X$	$\frac{cz(1+z)}{D_L}$
A1254	132.38	+44.47	−0.70170	0.0628	17.0	220.08	−20.520	−0.5750	44.5
A1257	183.42	+70.05	−0.86027	0.0339	15.0	138.56	−21.203	−0.7579	65.6
A1278	228.30	+70.30	−0.82100	0.129	17.3	366.23	−21.922	−0.5919	61.2
A1401	170.21	+73.90	−0.81044	0.1648	17.0	424.86	−22.805	−0.5552	77.6
A1413	226.36	+76.79	−0.77526	0.1427	17.1	388.38	−22.348	−0.5482	70.5
A1437	273.62	+63.27	−0.64208	0.1339	17.2	368.88	−22.056	−0.4618	66.3
A1514	251.37	+79.98	−0.70680	0.1995	17.6	470.54	−22.645	−0.4652	62.9
A1525	287.73	+60.86	−0.54366	0.259	18.0	536.29	−22.863	−0.3378	55.5
A1548	268.03	+80.74	−0.67039	0.1611	17.5	414.38	−22.209	−0.4635	62.1
A1550	133.40	+68.97	−0.73072	0.254	17.8	537.20	−23.061	−0.4536	59.2
A1571	123.59	33.76	−0.56024	0.209	17.6	477.90	−22.721	−0.3664	64.7
A1674	121.16	+49.59	−0.62765	0.1055	17.2	315.39	−21.488	−0.4730	58.5
A1758	107.16	+65.34	−0.59621	0.280	18.0	560.17	−23.078	−0.3627	55.2
A1759	359.94	+78.08	−0.47614	0.168	17.6	418.31	−22.156	−0.3280	61.5
A1760	359.88	+78.04	−0.47558	0.1711	17.2	422.90	−22.600	−0.3264	74.4
A1763	92.61	+73.48	−0.56952	0.187	17.7	448.85	−22.346	−0.3821	60.1
A1918	106.42	+50.86	−0.51053	0.1415	17.5	377.51	−21.848	−0.3645	59.9
A1934	44.86	+67.48	−0.33932	0.2195	17.4	483.66	−22.986	−0.2208	73.6
A1940	96.15	+56.23	−0.46882	0.1396	17.0	372.94	−22.303	−0.3360	75.3
A1942	355.12	+55.28	−0.11802	0.224	17.5	481.87	−22.879	−0.0769	72.4
A1957	49.16	+65.35	−0.31984	0.241	17.8	508.65	−22.819	−0.2036	62.2
A1961	49.09	+65.05	−0.31519	0.232	17.8	497.98	−22.720	−0.2025	61.9

Table A3

Cluster	l	b	$-\cos\gamma$	z	m_{10}	r_z	$M_{1_{n=+1}}$	$-X$	$\frac{cz(1+z)}{D_L}$
A1990	42.12	+62.96	−0.26256	0.1269	17.2	344.32	−21.813	−0.1929	66.7
A2100	60.46	+53.95	−0.20349	0.1533	17.0	386.76	−22.454	−0.1441	80.4
A2111	54.96	+53.41	−0.16611	0.229	17.8	489.48	−22.648	−0.1075	63.0
A2204	21.10	+33.24	+0.28474	0.1523	17.1	370.01	−22.201	+0.2046	79.9
A2224	30.87	+34.35	+0.24565	0.1504	17.4	368.18	−21.880	+0.1768	69.0
A2240	97.67	+36.24	−0.30117	0.138	17.4	364.82	−21.826	−0.2174	63.2
A2246	94.43	+36.19	−0.26613	0.225	17.6	487.96	−22.829	−0.1725	68.0
A2317	100.03	+23.74	−0.19803	0.211	17.6	468.32	−22.648	−0.1306	67.7
A2397	59.74	−39.15	+0.82779	0.224	17.9	452.28	−22.241	+0.5537	66.9
A2554	41.62	−66.79	+0.86066	0.106	16.9	274.21	−21.354	+0.6724	74.0
A2623	90.68	−52.41	+0.62492	0.1784	17.2	398.73	−22.406	+0.4380	84.1
A2632	75.31	−65.04	+0.74287	0.186	17.8	405.83	−21.882	+0.5174	65.5
A2646	75.65	−66.21	+0.73963	0.193	17.6	415.43	−22.177	+0.5109	72.8
A2658	73.28	−68.50	+0.74567	0.185	17.4	404.37	−22.267	+0.5200	78.6
A2670	81.33	−68.52	+0.71076	0.0745	15.7	213.39	−21.756	+0.5858	98.2
A2694	102.81	−52.52	+0.52791	0.0958	17.0	262.83	−21.106	+0.4166	64.7
A2721	352.11	−77.69	+0.77847	0.114	17.0	291.15	−21.453	+0.5993	73.8
A2744	8.91	−81.24	+0.75130	0.308	17.4	544.69	−23.609	+0.4633	87.3
A3128	264.74	−51.11	+0.33377	0.0554	15.3	176.08	−21.584	+0.2844	91.1
A3559	312.87	+32.60	−0.04463	0.0471	15.7	161.78	−20.939	−0.0385	65.1
A3855	8.48	−56.33	+0.95691	0.1214	17.2	299.72	−21.358	+0.7311	70.8
S0910	330.40	−37.66	+0.82453	0.311	17.4	545.33	−23.619	+0.5082	88.1